J. Biochem. 119, 703-710 (1996)

Effects of Point Mutations at the Flexible Loop Glycine-67 of *Escherichia coli* Dihydrofolate Reductase on Its Stability and Function

Eiji Ohmae, Koji Iriyama, Shigeyuki Ichihara, and Kunihiko Gekko[1]

Department of Applied Biological Science, Faculty of Agriculture, Nagoya University, Chikusa-ku, Nagoya, Aichi 464-01

Received for publication, October 11, 1995

To elucidate the role of a flexible loop (residues 64-72) in the stability and function of *Escherichia coli* dihydrofolate reductase, glycine-67 in this loop was substituted by site-directed mutagenesis with seven amino acids (Ala, Cys, Asp, Leu, Ser, Thr, and Val). The circular dichroism spectra suggested that the conformation of the native structure was affected by the mutations in both the presence and absence of NADPH. The free energy change of unfolding by urea decreased in the order of G67A > G67S ≧ wild-type ≧ G67D > G67T > G67C ≧ G67L > G67V. The steady-state kinetic parameters for the enzyme reaction, K_m and k_{cat}, were only slightly influenced, but the rate of the hydride transfer reaction was significantly changed by the mutations, as revealed by the deuterium isotope effect on the enzyme activity. These results suggest that site 67 in the flexible loop, being very far from the active site, plays an important role in the stability and function of this enzyme. The characteristics of the mutations were discussed in terms of the modified flexibility of the native structure, compared with the results of mutations at site 121 in another flexible loop [Gekko *et al.* (1994) *J. Biochem.* 116, 34-41].

Key words: dihydrofolate reductase, enzyme function, point mutation, role of flexible loop, structural stability.

In order to elucidate the structure-function relationships of proteins or enzymes, many mutation studies have been carried out focusing on the positions at or around the active site, the hydrophobic core, and the secondary structure. There are relatively small number of reports on amino acid substitutions in flexible loops, but they suggested the important role of loop regions in the stability and function of some enzymes (*1-5*). Hedstrom *et al.* found that trypsin can be converted to a chymotrypsin-like protease through changes in the surface loops (*1*). Oda *et al.* showed that the catalytic reaction of glutathione synthetase is modified by mutations in its flexible loops (*2-4*). The rate of hydride-transfer from NADPH to the substrate, dihydrofolate, decreases markedly when four residues (Met16-Ala19) in the most mobile loop of dihydrofolate reductase (residues 9-24) are replaced by a glycine (*5*). However, it has not been clearly explained why mutations in flexible loops affect the stability and function of enzymes, although the modified flexibility of the structure is expected to be a main factor. The answer to this question should provide a new insight into the principles of protein folding, the structure-function relationships of enzymes, and protein engineering.

Dihydrofolate reductase (DHFR) from *Escherichia coli* is an excellent example for studying the structure-flexibility-function relationships of enzymes. DHFR has several flexible loops such as residues 9-24, 64-72, 117-131, and 142-149, as revealed by the large B-factor of X-ray crystallographic data (*6-8*). In the previous studies, we showed that site-directed mutagenesis at glycine-121 in a flexible loop (residues 117-131) significantly influences the stability and enzyme function despite that the α-carbon at this site is 19 Å apart from catalytic residue Asp27 (*9, 10*). Interestingly, we recently found that the adiabatic compressibility of these mutants increases as the stability and enzyme activity decrease (Gekko *et al.*, to be published). These findings predict that the flexible loop has a dominant effect on the flexibility, stability and function of this enzyme, this being consistent with the result of X-ray analysis that the mobility of this loop is largely depressed on the binding of an inhibitor, methotrexate (*6, 8*). Modified flexibility of the structure has also been assumed for mutants at the hinge region, Val88 (*11*), and at residues 16-19 in a flexible loop (residues 9-24) (*5*).

In the present study, to elucidate the role of another flexible loop (residues 64-72) connecting the βC and βD strands, we constructed seven mutants as to glycine 67, one of the most mobile residues in this loop. The α-carbon at this site is 29.3 Å apart from catalytic residue Asp27, so this position will not directly participate in the enzyme reaction of DHFR like site 121. A characteristic of this loop is that the mobility increases (the B-factor increases) when methotrexate is bound, although that of other flexible loops decreases (*6, 8*). The effects of mutations at site 67 on the stability and function will be discussed in terms of the modified native structure, as compared with those of mutations at site 121 (*10*).

[1] To whom correspondence should be addressed at the present address: Department of Materials Science and Graduate Department of Gene Science, Faculty of Science, Hiroshima University, Kagamiyama, Higashi-Hiroshima 739.

Abbreviations: CD, circular dichroism; H_2F, dihydrofolate; DHFR, dihydrofolate reductase; MTX, methotrexate; H_4F, tetrahydrofolate.

MATERIALS AND METHODS

Plasmid and Mutant Constructions—All mutant DHFR genes were produced with plasmid pTP64-1 (5.3 kb) constructed by Iwakura and Tanaka (*12*), which was 840-fold overexpressed compared to in the case of non-plasmid cells for wild-type DHFR. The following seven oligonucleotides for mutants were synthesized with an Applied Biosystems DNA synthesizer Model 380A: 5′CGATCGTCCGTAGCCGGTTGACTGC3′ (G67A), 5′CGATCGTCCGTACACGGTTGACTGC3′ (G67C), 5′CGATCGTCCGTATCCGGTTGACTGC3′ (G67D), 5′CGATCGTCCGTAACCGGTTGACTGC3′ (G67V), 5′TCGTCCGTAGACGGTTGAC3′ (G67S), 5′TCGTCCGTAGGCGGTTGAC3′ (G67L), and 5′TCGTCCGTAGTCGGTTGAC3′ (G67T). Mutant plasmids G67A, G67C, G67D, and G67V were constructed by site-directed mutagenesis from pTP64-1 by the gapped-duplex method, using a Mutan™-G kit (Takara). Mutant plasmids G67S, G67L, and G67T were constructed by the same method from the mutant plasmid of G67A. All mutant plasmids obtained were identified and confirmed by DNA sequence analysis using the dideoxy chain termination method (*13*).

Protein Purification—The wild-type and mutant DHFR proteins were purified according to the methods described previously (*9*), in which the gel filtration chromatography on Sephadex G-75 was replaced by fractionation with ammonium sulfate according to Ahrweiler and Frieden (*11*). The concentration of wild-type DHFR was determined using a molar extinction coefficient of 31,100 $M^{-1}\cdot cm^{-1}$ at 280 nm (*14*). The concentrations of mutant DHFRs were determined assuming the same molar extinction coefficient since the amino acids introduced in this study have no or negligibly small chromophores.

Circular Dichroism Spectra—Circular dichroism (CD) spectra of the wild-type and mutant DHFRs were measured at 15°C using a Jasco J-720W spectropolarimeter. The solvent conditions were 10 mM potassium phosphate (pH 7.0) containing 0.1 mM EDTA and 0.1 mM dithiothreitol. The protein concentration was kept at about 20 μM. When holoenzymes were measured, 0.5 mM NADPH was added and preincubated for 30 min. For CD measurements of apoenzymes in a 6 M urea solution, the sample solutions were preincubated for over 10 h to allow complete unfolding of the enzymes.

Equilibrium Unfolding—Equilibrium unfolding of DHFRs with urea (ultrapure product from Schwarz/Mann) was monitored by means of CD measurements at 222 nm and 15°C with a Jasco J-40A spectropolarimeter as described previously (*9*). The solvent conditions were 10 mM potassium phosphate (pH 7.0) containing 0.1 mM EDTA and 1.4 mM 2-mercaptoethanol. The protein concentration was kept at about 10 μM. All samples were fully equilibrated at each denaturant concentration before the CD spectra were measured. The observed molar ellipticity data, $[\theta]$ (30-38 points), were directly fitted to the two-state unfolding model, native (N) $\rightleftharpoons$ unfolded (U), by means of nonlinear least-squares regression analysis with the SALS program (*15*), as follows

$$[\theta]=\{[\theta]_N+[\theta]_U\exp(-\Delta G_u/RT)\}/\{1+\exp(-\Delta G_u/RT)\} \quad (1)$$

where ΔG_u is the Gibbs free energy change of unfolding, R the gas constant, T the absolute temperature, and $[\theta]_N$ and $[\theta]_U$ the molar ellipticities of the native and unfolded forms, respectively. $[\theta]_N$ and $[\theta]_U$ at a given urea concentration were estimated by assuming the same linear dependence of ellipticity in the transition region as in the pure native (pre-transition region) and unfolded states (post-transition region). The free energy change of unfolding, ΔG_u, in Eq. 1 was assumed to be linearly dependent on the urea concentration (*16*)

$$\Delta G_u=\Delta G^{\circ}_u+m[\text{urea}] \quad (2)$$

where ΔG°_u is the free energy change of unfolding in the absence of a denaturant and the slope, m, is a parameter reflecting the cooperativity of the transition. The urea concentration at the mid point of the transition ($\Delta G_u=0$) was defined as C_m.

Steady-State Kinetics—The steady-state kinetics of the enzyme reaction were studied spectrophotometrically using a Jasco V-520 spectrophotometer at 25°C. The concentrations of dihydrofolate, H_2F (Sigma), and NADPH (Oriental Yeast) were determined spectrophotometrically using molar extinction coefficients of 28,000 $M^{-1}\cdot cm^{-1}$ at 282 nm and 6,200 $M^{-1}\cdot cm^{-1}$ at 339 nm, respectively. The enzyme concentrations were determined by the methotrexate titration method (*17*) to eliminate the effects of denatured species which may be produced during storage. The buffer used was 33 mM succinic acid containing 44 mM imidazole and 44 mM diethanolamine, whose pH was adjusted to 7.0 with acetic acid or tetraethylammonium hydroxide. The Michaelis constant (K_m) and the rate constant of catalysis (k_{cat}) for H_2F were measured with various concentrations of H_2F, 0.3 to 60 μM, at a saturated concentration of NADPH (60 μM). When these parameters were measured for NADPH, the concentration of H_2F was kept at 50 μM and that of NADPH was varied, 0.3-60 μM. The final concentrations of the enzymes were 0.5-1.5 nM. The enzyme solutions were preincubated with NADPH or H_2F for 10 min to eliminate the hysteresis effect (*18*), and the reaction was started by adding H_2F or NADPH to the preincubated mixture. The initial velocities (v) of the enzyme reaction were calculated from the time course of absorbance at 340 nm using a differential molar extinction coefficient of 11,800 $M^{-1}\cdot cm^{-1}$ (*19*). The K_m and k_{cat} values were determined with the following equation by nonlinear least-squares analysis with the SALS program

$$v=(k_{cat}[E][S])/(K_m+[S]) \quad (3)$$

where [E] is the enzyme concentration and [S] the initial substrate concentration.

Deuterium Isotope Effect—[4′(*R*)-^{2}H]NADPH (NADPD) was prepared by the method of Chen *et al.* (*20*) using *Leuconostoc mesenteroides* alcohol dehydrogenase (Research Plus). The obtained NADPD was purified by the method in the same report, followed by gel filtration chromatography on Bio-Gel P-2 (Bio-Rad) according to Viola *et al.* (*21*). The absence of chloride ions was confirmed by the HNO_3-$AgNO_3$ precipitation method. The enzyme activity was measured under the same conditions as described above using NADPD (60 μM) instead of NADPH. The kinetic parameters were obtained with Eq. 3 and the deuterium isotope effect, ^DV, was calculated with the following equation

$$^{D}V = k_{cat,NADPH}/k_{cat,NADPD} \quad (4)$$

where $k_{cat,NADPH}$ and $k_{cat,NADPD}$ are the k_{cat} values for H_2F when NADPH and NADPD are used as the coenzyme, respectively.

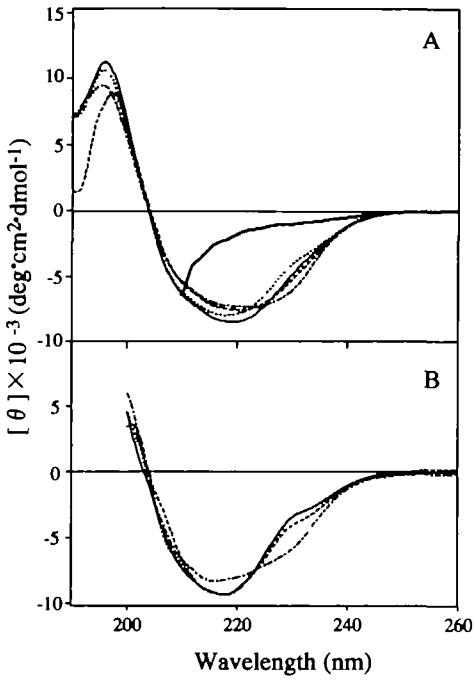

Fig. 1. **Far-ultraviolet circular dichroism spectra of the wild-type and three mutant DHFRs in the absence (A) or presence (B) of NADPH at 15°C.** The solvent used was 10 mM potassium phosphate (pH 7.0) containing 0.1 mM EDTA and 0.1 mM dithiothreitol. (—) Wild-type DHFR; (·····) G67S; (·····) G67T; (-·-·-) G67V. (—) in the panel A indicates the wild-type and mutant DHFRs in 6 M urea solutions.

RESULTS

Circular Dichroism Spectra—Figure 1 shows the far-ultraviolet CD spectra of the wild-type and three mutant DHFRs in the presence or absence of NADPH. The wild-type apo-DHFR gave a negative peak of −8,500 deg·cm²·dmol⁻¹ at 219 nm and a positive peak of 11,200 deg·cm²·dmol⁻¹ at 196 nm (Fig. 1A), which are consistent with the previous data (*9*). The spectra of G67C and G67D resembled that of wild-type DHFR, although the peak intensities were slightly different (data not shown). However, G67S showed a slightly but obviously different spectrum having a shoulder at around 235 nm, a negative peak of −8,000 deg·cm²·dmol⁻¹ at 218 nm, and a positive peak of 10,600 deg·cm²·dmol⁻¹ at 196 nm. Similar CD spectra were obtained for G67A and G67L (data not shown). On the other hand, G67T and G67V showed red-shifted negative peaks of −7,600 deg·cm²·dmol⁻¹ at 221 nm and −7,400 deg·cm²·dmol⁻¹ at 222 nm, respectively. These results suggest that the conformation of apo-DHFR was considerably modified

TABLE I. **Thermodynamic parameters for urea denaturation of the wild-type and mutant DHFRs at 15°C.**[a]

DHFRs	Δg^{*}_{tr}[b] (kcal/mol)	ΔG^{*}_{u}[c] (kcal/mol)	m[c] (kcal/mol·M)	C_m[c] (M)
Wild-type[d]	0.0	6.08±0.18	−1.96±0.06	3.11
G67S	−0.3	6.15±0.18	−2.18±0.06	2.82
G67A	0.5	6.60±0.08	−2.34±0.03	2.82
G67C	1.0	5.72±0.12	−2.05±0.04	2.79
G67D	−2.5	5.94±0.12	−2.27±0.04	2.62
G67V	1.5	5.14±0.17	−1.78±0.05	2.89
G67L	1.8	5.64±0.17	−1.99±0.06	2.83
G67T	0.4	5.87±0.05	−2.24±0.05	2.62

[a]The solvent used was 10 mM potassium phosphate (pH 7.0) containing 0.1 mM EDTA and 1.4 mM 2-mercaptoethanol. [b]The transfer free energy change of introduced amino acid side chains from organic solvent to water (*45*). [c]The parameters, ΔG^{*}_{u}, m, and C_m, were calculated assuming a linear relationship between ΔG_u and the urea concentration (Eq. 2). [d]Gekko *et al.* (*10*).

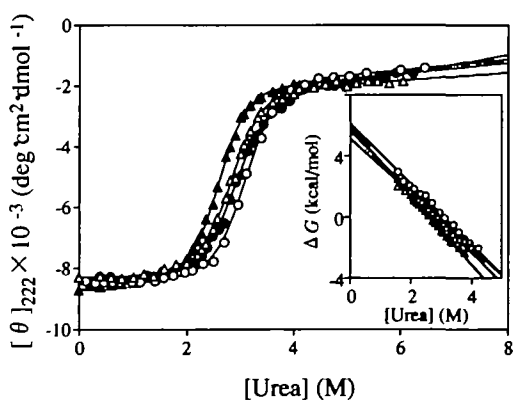

Fig. 2. **Plots of molar ellipticity of the wild-type and three mutant DHFRs at 222 nm as a function of the urea concentration at 15°C.** The solvent used was 10 mM potassium phosphate (pH 7.0) containing 0.1 mM EDTA and 1.4 mM 2-mercaptoethanol. (○) Wild-type DHFR; (●) G67V; (△) G67L; (▲) G67T. Solid lines represent the theoretical fits to a two-state model with the parameter values shown in Table I (see "MATERIALS AND METHODS"). The inset in the figure shows the dependence of ΔG_u on the urea concentration.

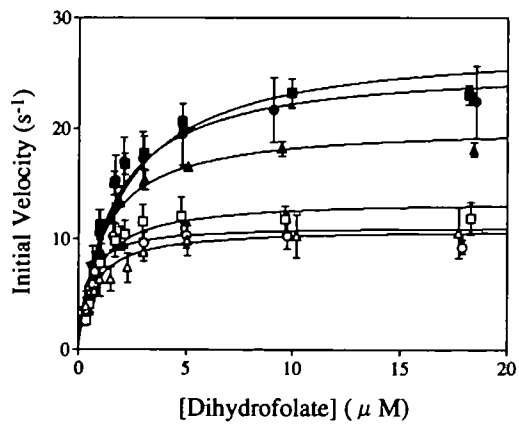

Fig. 3. **Initial velocity of the enzymatic reaction of the wild-type and two mutant DHFRs as a function of the dihydrofolate concentration at 25°C.** The solvent used was 33 mM succinic acid, 44 mM imidazole, and 44 mM diethanolamine (pH 7.0), containing 60 μM NADPH (closed symbols) or NADPD (open symbols). The concentrations of enzymes were 0.5-1.5 nM. (●, ○) Wild-type DHFR; (■, □) G67S; (▲, △) G67A. Solid lines represent the theoretical fits to Eq. 3 with the parameter values shown in Table II.

TABLE II. **Steady-state kinetic parameters and deuterium isotope effects for the enzyme activity of the wild-type and mutant DHFRs at 25°C.**[a]

DHFRs	For dihydrofolate		For NADPH		^{D}V[b]
	K_m (μM)	k_{cat} (s^{-1})	K_m (μM)	k_{cat} (s^{-1})	
Wild-type	1.3±0.1	24.6±3.1	1.1±0.3	22.9±3.8	2.2
G67S	1.4±0.1	26.4±1.3	0.9±0.1	21.2±4.0	1.6
G67A	1.1±0.1	20.0±0.7	1.0±0.1	18.5±1.2	1.8
G67C	1.2±0.1	24.6±3.6	1.7±0.2	21.2±3.0	3.0
G67D	1.2±0.2	20.6±2.5	2.3±0.5	18.0±0.9	3.0
G67V	1.3±0.5	19.1±1.7	1.1±0.3	17.3±3.2	2.6
G67L	1.1±0.1	22.6±3.7	0.8±0.2	18.2±1.6	1.6
G67T	1.8±0.4	26.6±3.1	1.2±0.1	21.0±1.0	1.6

[a]The solvent used was 33 mM succinic acid containing 44 mM imidazole and 44 mM diethanolamine (pH 7.0). [b]The deuterium isotope effect on k_{cat} calculated with Eq. 4.

by a mutation at site 67, as well as at site 121 (*9*).

When NADPH was added, a shoulder appeared at around 235 nm in the CD spectrum of wild-type DHFR (Fig. 1B). The spectra of G67S and G67T were very similar to that of wild-type DHFR, suggesting their conformations are essentially the same. However, G67V showed a considerably different spectrum with a flat and blue-shifted peak. This implies that a mutation at site 67 could influence the conformation of DHFR even in the holoenzyme.

To obtain information on the unfolded conformation, the CD spectra of apo-DHFRs were measured in a 6 M urea solution. As shown in Fig. 1A, the spectrum of any mutant examined overlapped that of wild-type DHFR, suggesting that the conformation of unfolded DHFR may be essentially identical in any mutant.

Equilibrium Unfolding—Figure 2 shows typical plots of the molar ellipticities at 222 nm of the wild-type and three mutant DHFRs as a function of the urea concentration at 15°C. Similar transition curves were observed for other mutant DHFRs. The CD spectra of G67S, G67L, and G67T at various urea concentrations exhibited an isoellipticity point at 210 nm and the same transition curve, respectively, at any wavelength in the range of 200-260 nm (data not shown). This indicates that the unfolding of the mutant DHFRs essentially follows the two-state model, as in the case of wild-type DHFR and other mutants (*22-24*). The free energy change of unfolding, ΔG_u, was calculated with Eq. 1 and plotted against the urea concentration in the inset in Fig. 2. The good linear relationship observed allows us to calculate the free energy change of unfolding in water, ΔG°_u, the slope, m, and the denaturant concentration at $\Delta G_u = 0$, C_m. The results of the calculation are listed in Table I. Evidently, these parameters are dependent on the amino acid introduced: the stability decreased in the order of G67A > G67S ≧ wild-type ≧ G67D > G67T > G67C ≧ G67L > G67V.

The m values changed almost in parallel with ΔG°_u (correlation coefficient, r, between the two parameters, 0.795). Except for G67V, any mutant showed higher cooperativity of transition compared with wild-type DHFR. On the other hand, the C_m values of all mutants were smaller than that of wild-type DHFR, and there was no correlation between C_m and ΔG°_u ($r = 0.001$).

Steady-State Kinetics—Figure 3 shows typical plots of the initial velocity of the enzyme reaction as a function of the substrate concentration (H_2F). Similar hyperbolic curves were observed for other mutant DHFRs. This was also the case with the plots of initial velocity *versus* NADPH concentration. The Michaelis constant, K_m, and the rate constant of catalysis, k_{cat}, were calculated using Eq. 3 and are listed in Table II. The K_m and k_{cat} values of wild-type DHFR for H_2F and NADPH were consistent with the data reported by another group (*25*), although the k_{cat} values seemed slightly smaller. The K_m values of the mutants for H_2F varied in the range of 1.1 μM (G67A and G67L) to 1.8 μM (G67T), and the k_{cat} values in the range of 19.1 s^{-1} (G67V) to 26.6 s^{-1} (G67T), which are not greatly different from those of wild-type DHFR. These results are considerably different from those for mutations at site 121, which showed a large decrease in k_{cat} although the K_m value was almost constant (*10*). The K_m and k_{cat} values for NADPH were also not significantly changed by the mutations, although G67C and G67D showed slightly larger K_m values compared with wild-type DHFR. From these results, it seems that site 67 does not play so important a role as site 121 in the enzyme function of DHFR. To examine this further, we determined the deuterium isotope effects on the kinetic parameters.

Deuterium Isotope Effect—As shown in Fig. 3, the initial velocity of the enzyme reaction was depressed for most mutants when NADPD was used instead of NADPH. This is predominantly ascribed to the large decrease in k_{cat} since K_m did not change. The deuterium isotope effects on k_{cat}, ^{D}V, calculated using Eq. 4, are listed in the last column of Table II. The ^{D}V values of G67C and G67D were 3.0, suggesting that the hydride transfer from NADPH to H_2F was fully rate-determining for these mutants. In contrast, the hydride transfer was only partially rate-determining for the three mutants, G67S, G67L, and G67T, for which $^{D}V = 1.6$. These results indicate that the rate of the hydride transfer reaction was affected by a mutation at site 67, although the apparent kinetic parameters were not greatly changed.

DISCUSSION

As shown in this study, a mutation at site 67 brought about considerably large changes in the native structure and stability, but only small changes in the enzyme function. These results imply the importance of this site as well as site 121 for DHFR although they are located in flexible loops far from the active site. A matter of concern is how such a local change in the primary structure of a flexible loop is coupled to the stability and function of the overall protein structure. This problem will be discussed below on the basis of the statistical analyses of the results, as compared with those for mutations at site 121 (*10*).

Structure of Mutant DHFRs—As shown in Fig. 1A, the CD spectrum of apo-DHFR was obviously affected by mutations at site 67. The CD spectrum of holo-DHFR was also modified by the mutations although the conformational change was suppressed, to some extent, on the binding of NADPH (Fig. 1B). We previously found that the CD spectrum of apo-DHFR was influenced by mutations at site 121 (*9, 10*), and there have been some reports of the same context by other groups (*11, 26*). It is not probable that the content of the secondary structure is changed by the mutations since all mutants in this study had comparable activities to wild-type DHFR (Table II). Such a large

modification of the CD spectrum may be rather ascribed to a highly flexible structure of DHFR, which could perturb the CD excitation through some movement of the secondary structure and/or altered contributions of aromatic side chains (*27-31*). Kuwajima *et al.* (*26*) proposed that wild-type DHFR has an exciton pair of two aromatic residues, Trp74 and Trp47, contributing to the peptide CD, since the replacement of Trp74 by leucine led to a large change in the CD spectrum. Figure 4B shows the distances between the α-carbon of Gly67 and the residual atoms of Trp74 in the DHFR-MTX complex (B-chain) (*6*). The distance to the nearest atom, ε_2-carbon, is only 3.41 Å. Therefore, it is possible that a mutation at site 67 influences the surroundings of the side chain of Trp74 thereby disrupting the exciton with Trp47. This may be supported by that the CD spectrum of G67V greatly resembles that of the W74L mutant. A detailed understanding of the structural changes, however, must await X-ray or NMR analyses of the mutant enzymes.

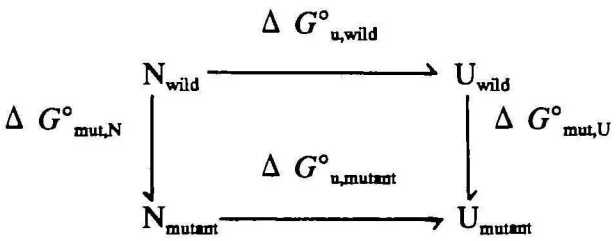

Scheme 1

When DHFRs were sufficiently unfolded in a 6 M urea solution, any mutants showed the same CD spectra as wild-type DHFR. This suggests that the conformation of the unfolded form would not be substantially affected by mutations at site 67, although there may be some residual structure (*32*). These results are consistent with those of a recent kinetic refolding study, which predicted four native conformers and only one unfolded conformer (*33*).

Structural Stability—As shown in Table I, the free energy change of unfolding in water, ΔG°_{u}, was influenced by mutations at site 67. Large changes in ΔG°_{u} were also observed for mutations at site 121 (*9, 10*). It is of interest that the highly mobile sites located in the flexible loops play an important role in the structural stability of DHFR. The mutation effects on the stability can be quantitatively analyzed with free energy diagram (Scheme 1); where N and U are the native and unfolded states, respectively, and $\Delta G^{\circ}_{mut,N}$ and $\Delta G^{\circ}_{mut,U}$ denote the free energy changes of mutation (amino acid substitution) in the native and unfolded states, respectively. According to this diagram,

$$\Delta\Delta G^{\circ}_{u} = \Delta G^{\circ}_{u,mutant} - \Delta G^{\circ}_{u,wild} = \Delta G^{\circ}_{mut,U} - \Delta G^{\circ}_{mut,N} \quad (5)$$

There are many experimental data showing that $\Delta\Delta G^{\circ}_{u}$ is proportional to the hydrophobicity of introduced amino acid side chains (*34-37*), this being consistent with a consensus that the hydrophobic interaction is the dominant stabilizing force for the native protein structure (*38*). However, some discrepancies have been found with λ repressor protein (*39*), staphylococcal nuclease (*40-42*), and DHFR (*24*). It is known that the protein structure is oppositely destabilized by introducing nonpolar residues to a surface amino acid of λ-*Cro* protein (*43*) and cytochrome *c* (*44*). These results demonstrate that the effects of mutations are highly site-dependent.

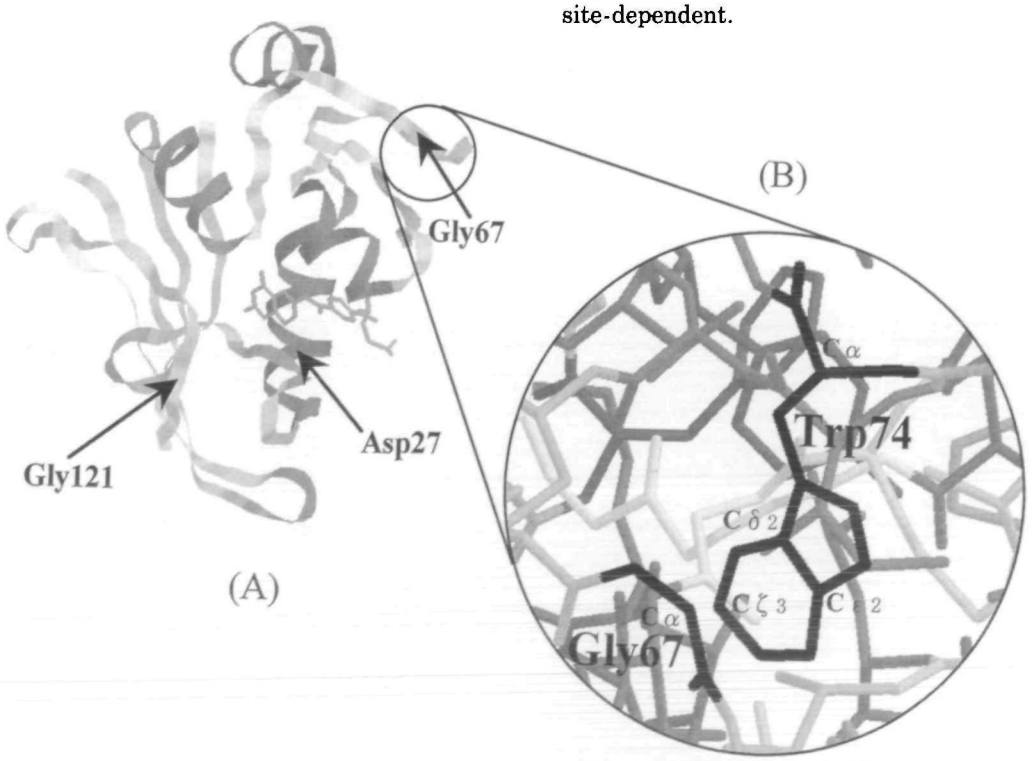

Fig 4. **The overall structure (A), and an expanded picture around Gly67 and Trp74 (B) of a DHFR-MTX binary complex (B-chain) (*6*).** (A) The positions of Gly67, Gly121, and Asp27, an active site residue, are indicated by arrows. (B) The distances from the α-carbon of Gly67 to the α, δ_2, ε_2, and ζ_3-carbons of Trp74 are 6.07, 3.46, 3 41, and 4 28 Å, respectively.

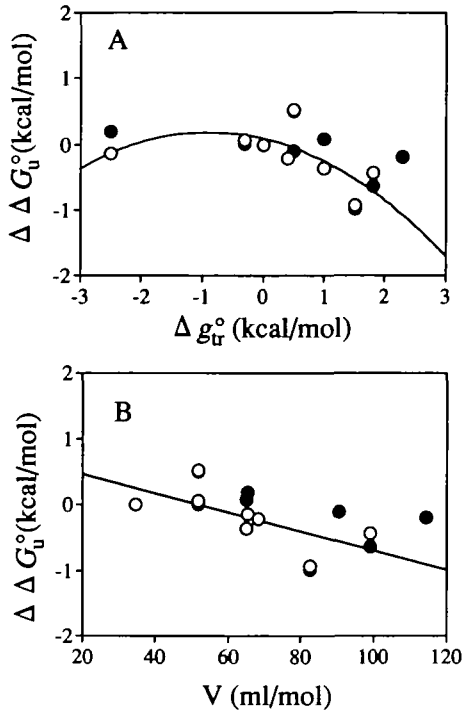

Fig. 5. **Plots of $\Delta\Delta G^{\circ}_{u}$ against the hydrophobicity (A) and the molar volume (B) of introduced amino acid side chains for the wild-type and mutant DHFRs at sites 67 (○) and 121 (●).** The $\Delta\Delta G^{\circ}_{u}$ values were calculated with Eq. 5. The hydrophobicity, Δg°_{tr}, is cited from Nozaki and Tanford (*45*). The molar volume, V, is cited from Zamyatnin (*51*). The solid lines were drawn by the least-squares method.

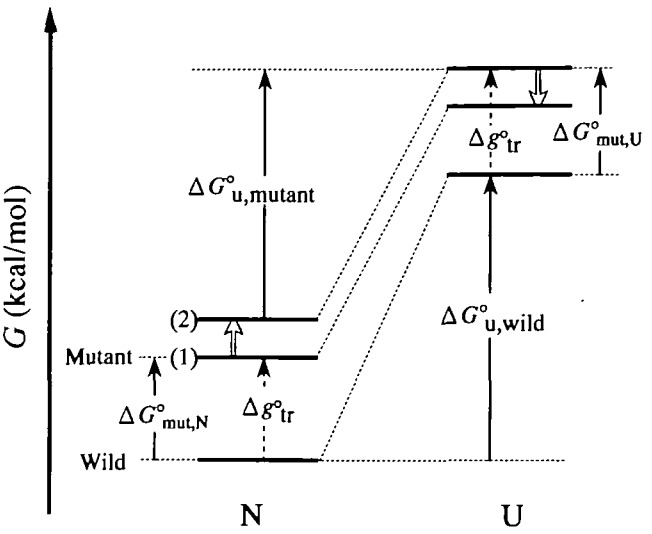

Scheme 2. **Mutation effects on the free energy level (G) of native (N) and unfolded (U) states of protein.** The reverse hydrophobic effect on the stability is assumed to result from two typical situations: (1) the depressed free energy increase of U-state due to enhanced hydrophobic interaction (downward empty arrow) and (2) the enhanced free energy increase of N-state (upward empty arrow) due to modification of native structure (atomic overcrowding). The numbers (1) and (2) in the scheme correspond to above two situations.

Figure 5 shows plots of the $\Delta\Delta G^{\circ}_{u}$ values, which were calculated from the results in Table I, as a function of the hydrophobicity (Δg°_{tr}) estimated by Nozaki and Tanford (*45*), and the molar volume (V) of introduced amino acid side chains at site 67. The results for the site 121 mutants in the previous study (*10*) are also plotted in this figure for comparison. Although the correlation is low, $\Delta\Delta G^{\circ}_{u}$ seems to be a decreasing function of Δg°_{tr}, as found for the site 121 mutants. Thus, the effects of mutations at site 67 on the stability cannot be explained in terms of the enhanced hydrophobic interaction of the native structure. There are two possible explanations, as a typical case, for such a reverse hydrophobic effect on the stability. The first is that the nonpolar side chains introduced are less exposed to the solvent in the unfolded state than in the native state, resulting in stabilization of the hydrophobic interaction of the unfolded state (*43, 44*). This means that $\Delta G^{\circ}_{mut,U}$ is smaller than $\Delta G^{\circ}_{mut,N}$ because of the depressed free energy increase in the unfolded state, which would be brought about by the large entropy increase due to dehydration around the nonpolar groups introduced (Scheme 2). This may be possible for a mutation at a hyper or highly exposed position (*43, 44*), but there is no direct experimental evidence supporting this idea, even if the unfolded conformation is different with the mutants, as found for staphylococcal nuclease (*41*). NMR and compressibility studies rather suggest that the amino acid side chains of unfolded proteins are fully exposed to the solvent as well as small model compounds (*46, 47*). If this is the case, the dominant effect of a mutation must be attributed to the native state. Some change in the native structure must occur to induce the large positive value of $\Delta G^{\circ}_{mut,N}$ overcoming $\Delta G^{\circ}_{mut,U}$, the latter corresponding to the free energy increase brought about on the introduction of nonpolar amino acid residues, $\Delta^{\circ}g_{tr}$ (Scheme 2). From the thermodynamics, however, it is *a priori* difficult to determine which of the native and unfolded structures predominantly contributes to the modified stability of mutants, since $\Delta G^{\circ}_{mut,N}$ and $\Delta G^{\circ}_{mut,U}$ or the corresponding heat capacity changes are generally unknown.

As suggested by the CD spectra (Fig. 1), the native structure of DHFR is sensitively influenced by mutations at site 67, while the unfolded conformation seems to be essentially identical. Therefore, it is not unreasonable to assume that the reverse hydrophobic effect of mutations observed is mainly caused by the modified native structure. The negative correlation between $\Delta\Delta G^{\circ}_{u}$ and the molar volume of amino acids (V) (Fig. 5B) suggests that the bulkiness of the side chains at site 67 as well as at 121 may be rather responsible for destabilization of the native structure. According to computer simulation, glycine at sites 67 and 121 cannot be substituted with any other amino acid without accompanying movement of the backbone polypeptide chain (Segawa, S., personal communication). Therefore, it is probable that overcrowding of the bulky side chain may strain the backbone chain conformation, leading to a decrease in the packing density of the overall structure. This is supported by our recent finding that ΔG°_{u} of mutants at site 121 decreases with increasing adiabatic compressibility of the native structure (Gekko *et al.*, to be published). The compressibility measurements of the mutants as to site 67, in progress in our laboratory, could confirm the above overcrowding hypothesis, since com-

pressibility can sensitively reflect the atomic packing of the native structure (*48*). It is noteworthy that such overcrowding of side chains predominantly contributes to the reverse hydrophobic effect on the stability of mutants as to Val88, the central residue in the hinge region (residues 85-91) of DHFR (*11*).

A noticeable finding is that ΔG°_{u} increases in proportion to the *m* value, while it is not dependent on C_m (Table I). Similar results were obtained for the mutants as to site 121: *r* was 0.72 and 0.40 for *m* and C_m, respectively (*10*). Although interpretation of the *m* value remains controversial (*49, 50*), these results might constitute evidence that the stability of these mutants as to flexible sites is predominantly determined by the modified cooperativity of unfolding, which would be directly related to the flexibility of the native structure. A definite correlation between ΔG°_{u} and *m* was also found for many mutants of staphylococcal nuclease (*40-42*).

Enzyme Function—As shown in Table II, the kinetic parameters of mutant DHFRs at site 67 were not markedly different from those of wild-type DHFR. Considering the large differences in the stability of these mutants, it is interesting that the enzyme activity was not so much influenced by the mutations. A possible origin of this discrepancy may be that the stability was measured without ligands, but the activity was measured with NADPH and H_2F. As shown in Fig. 1, the variation of CD spectra on mutation is smaller for holoenzymes (DHFR-NADPH binary complexes) than for apoenzymes. Then, it may be expected that the structure of DHFR-NADPH-H_2F ternary complexes is not so significantly modified by the mutations as to affect the kinetic parameters. In this respect, it is noteworthy that the K_m value was almost constant but k_{cat} greatly decreased with mutations at site 121, despite that the stability was similarly influenced by mutations at site 67. This suggests that site 67 is not as important as site 121 for the enzymatic function of DHFR, although both sites have comparable importance in the structural stability (Fig. 5). This may be partly due to the long distance of site 67 (29.3 Å) from the active site, Asp27, compared with that of site 121 (19 Å).

Although the apparent activity is not significantly influenced by mutations at site 67, subtle variations can be seen in the K_m and k_{cat} values (Table II). This predicts that there may be some modified processes in the enzyme kinetics. According to Fierke *et al.* (*14*), the rate-determining step of the enzyme reaction for wild-type DHFR is the process of release of the product (H_4F) from the DHFR-NADPH-H_4F complex at neutral pH. As the pH increases, the hydride transfer from NADPH to H_2F is depressed and finally it becomes the rate-determining step at pHs above 8.4, leading to a 3-fold decrease in k_{cat} for NADPD compared with that for NADPH. Therefore, the deuterium isotope effect for k_{cat}, ^{D}V, may be a useful measure for determining whether or not the hydride transfer process is influenced by mutations. As shown in Table II, the hydride transfer is fully rate-determining for G67C and G67D ($^{D}V = 3$), while it is only partially rate-determining for the wild-type and other mutants. Although it is difficult to decide what the main factor affecting the hydride transfer is, the low affinity of NADPH for G67C and G67D, as revealed by the large K_m values, may partly contribute to the depression of this process. The pH profile of k_{cat} should be determined for further detailed understanding of the mutation effects, taking into consideration the ionization state (pK_a) of Asp27 in the active site.

As demonstrated in this study, site-directed mutagenesis of glycine at site 67, located in a flexible loop (residues 64-72), has a large effect on the stability, and a small effect on the apparent activity of *E. coli* DHFR. However, the hydride transfer reaction was greatly influenced, although this position is far (29.3 Å) from the active site Asp27. The similar effects of mutations at sites 67 and 121 on the stability suggest that the two flexible loops (residues 64-72 and 117-131) play important roles in the stability of this enzyme, although site 67 is not as important as site 121 for the enzyme function. The reverse hydrophobic and volume effects on the stability suggest that the main effect of these mutations is modification of the packing of the side chains, which affects the flexibility of the loop or the long-range molecular dynamics. A further insight into the long-range interaction should be obtained through a study in progress on the combination effects (additivity) of double mutants at sites 67 and 121, separated by 27.4 Å.

We wish to thank Dr. M. Iwakura of the National Institute of Bioscience and Human Technology for the gift of plasmid pTP64-1 and the helpful discussion, and Prof. K. Yoshikawa of Nagoya University for the use of the J-720W spectropolarimeter. We also thank the Nagoya University Computer Center for the use of the SALS program.

REFERENCES

1. Hedstrom, L., Szilagyi, L., and Rutter, W.J. (1992) Converting trypsin to chymotrypsin: The role of surface loops. *Science* **255**, 1249-1253
2. Tanaka, T., Kato, H., Nishida, T., and Oda, J. (1992) Mutational and proteolytic studies on a flexible loop in glutathione synthetase from *Escherichia coli* B: The loop and arginine 233 are critical for the catalytic reaction. *Biochemistry* **31**, 2259-2265
3. Tanaka, T., Yamaguchi H., Kato, H., Nishioka, T., Katsube, Y., and Oda, J. (1993) Flexibility impaired by mutations revealed the multifunctional roles of the loop in glutathione synthetase. *Biochemistry* **32**, 12398-12404
4. Kato, H., Tanaka, T., Yamaguchi, H., Hara, T., Nishioka, T., Katsube, Y., and Oda, J. (1994) Flexible loop that is novel catalytic machinery in a ligase. Atomic structure and function of the loopless glutathione synthetase. *Biochemistry* **33**, 4995-4999
5. Li, L., Falzone, C.J., Wright, P.E., and Benkovic, S.J. (1992) Functional role of a mobile loop of *Escherichia coli* dihydrofolate reductase in transition-state stabilization. *Biochemistry* **32**, 7826-7833
6. Bolin, J.T., Filman, D.J., Matthews, D.A., Hamlin, R.C., and Kraut, J. (1982) Crystal structures of *Escherichia coli* and *Lactobacillus casei* dihydrofolate reductase refined at 1.7 A resolution. *J. Biol. Chem.* **257**, 13650-13662
7. Bystroff, C., Oatley, S.J., and Kraut, J. (1990) Crystal structures of *Escherichia coli* dihydrofolate reductase: The $NADP^+$ holoenzyme and the folate·$NADP^+$ ternary complex. Substrate binding and a model for the transition state. *Biochemistry* **29**, 3263-3277
8. Bystroff, C. and Kraut, J. (1991) Crystal structure of unliganded *Escherichia coli* dihydrofolate reductase: Ligand-induced conformational changes and cooperativity in binding. *Biochemistry* **30**, 2227-2239
9. Gekko, K., Yamagami, K., Kunori, Y., Ichihara, S., Kodama, M., and Iwakura, M. (1993) Effects of point mutations in a flexible loop on the stability and enzymatic function of *Escherichia coli* dihydrofolate reductase. *J. Biochem.* **113**, 74-80
10. Gekko, K., Kunori, Y., Takeuchi, H., Ichihara, S., and Kodama, M. (1994) Point mutations at glycine-121 of *Escherichia coli* dihydrofolate reductase: Important roles of a flexible loop in the stability and function. *J. Biochem.* **116**, 34-41

11. Ahrweiler, P.M. and Frieden, C. (1991) Effects of point mutations in a hinge region on the stability, folding, and enzymatic activity of *Escherichia coli* dihydrofolate reductase. *Biochemistry* **30**, 7801-7809
12. Iwakura, M. and Tanaka, T. (1992) Dihydrofolate reductase gene as a versatile expression marker. *J. Biochem.* **111**, 31-36
13. Sanger, F., Nicklen, S., and Coulson, A.R. (1977) DNA sequencing with chain-terminating inhibitors. *Proc. Natl. Acad. Sci. USA* **74**, 5463-5467
14. Fierke, C.A., Johnson, K.A., and Benkovic, S.J. (1987) Construction and evaluation of the kinetic scheme associated with dihydrofolate reductase from *Escherichia coli*. *Biochemistry* **26**, 4085-4092
15. Nakagawa, T. and Oyanagi, Y. (1980) Program system SALS for nonlinear least-squares fitting in experimental sciences in *Recent Developments in Statistical Inference and Data Analysis* (Matsushita, K., ed.) pp. 221-225, North Holland Publishing, Amsterdam
16. Pace, C.N. (1985) Determination and analysis of urea and guanidine hydrochloride denaturation curves in *Methods in Enzymology* (Hirs, C.H.W. and Timasheff, S.N., eds.) Vol. 131, pp. 267-280, Academic Press, New York
17. Williams, J.W., Morrison, J.F., and Duggleby, R.G. (1979) Methotrexate, a high-affinity pseudosubstrate of dihydrofolate reductase. *Biochemistry* **18**, 2567-2573
18. Penner, M.H. and Frieden, C. (1985) Substrate-induced hysteresis in the activity of *Escherichia coli* dihydrofolate reductase. *J. Biol. Chem.* **260**, 5366-5369
19. Stone, S.R. and Morrison, J.F. (1982) Kinetic mechanism of the reaction catalyzed by dihydrofolate reductase from *Escherichia coli*. *Biochemistry* **21**, 3757-3765
20. Chen, J.T., Taira, K., Tu, C.D., and Benkovic, S.J. (1987) Probing the functional role of phenylalanine-31 of *Escherichia coli* dihydrofolate reductase by site-directed mutagenesis. *Biochemistry* **26**, 4093-4100
21. Viola, R.E., Cook, P.F., and Cleland, W.W. (1979) Stereoselective preparation of deuterated reduced nicotinamide adenine nucleotides and substrates by enzymatic synthesis. *Anal. Biochem.* **96**, 334-340
22. Touchette, N.A., Perry, K.M., and Matthews, C.R. (1986) Folding of dihydrofolate reductase from *Escherichia coli*. *Biochemistry* **25**, 5445-5452
23. Perry, K.M., Onuffer, J.J., Touchette, N.A., Herndon, C.S., Gittelman, M.S., Matthews, C.R., Chen, J.T., Mayer, R.J., Taira, K., Benkovic, S.J., Howell, E.E., and Kraut, J. (1987) Effect for single amino acid replacements on the folding and stability of dihydrofolate reductase from *Escherichia coli*. *Biochemistry* **26**, 2674-2682
24. Garvey, E.P. and Matthews, C.R. (1989) Effects of multiple replacements at a single position on the folding and stability of dihydrofolate reductase from *Escherichia coli*. *Biochemistry* **28**, 2083-2093
25. Howell, E.E., Booth, C., Farnum, M., Kraut, J., and Warren, M.S. (1990) A second-site mutation at phenylalanine-137 that increases catalytic efficiency in the mutant aspartate-27→serine *Escherichia coli* dihydrofolate reductase. *Biochemistry* **29**, 8561-8569
26. Kuwajima, K., Garvey, E.P., Finn, B.E., Matthews, C.R., and Sugai, S. (1991) Transient intermediates in the folding of dihydrofolate reductase as detected by far-ultraviolet circular dichroism spectroscopy. *Biochemistry* **30**, 7693-7703
27. Dion, A., Linn, C.E., Bradrick, T.D., Georghiou, S., and Howell, E.E. (1993) How do mutations at phenylalanine-153 and isoleucine-155 partially suppress the effects of the aspartate-27→serine mutation in *Escherichia coli* dihydrofolate reductase? *Biochemistry* **32**, 3479-3487
28. Brahms, S. and Brahms, J. (1980) Determination of protein secondary structure in solution by vacuum ultraviolet circular dichroism. *J. Mol. Biol.* **138**, 149-178
29. Applequist, J. (1982) Theoretical π-π^* absorption and circular dichroic spectra of polypeptide β-structures. *Biopolymers* **21**, 779-795
30. Woody, R.W. (1985) Circular dichroism of polypeptides. *Peptides* **7**, 15-114
31. Sondek, J. and Shortle, D. (1992) Structure and energetic differences between insertions and substitutions in staphylococcal nuclease. *Proteins: Struct. Funct. Genet.* **13**, 132-140
32. Yang, J.T., Wu, C.C., and Martinez, H.M. (1986) Calculation of protein conformation from circular dichroism in *Methods in Enzymology* (Hirs, C.H.W. and Timasheff, S.N., eds.) Vol. 130, pp. 208-269, Academic Press, New York
33. Jones, B.E., Jennings, P.A., Pierre, R.A., and Matthews, C.R. (1994) Development of nonpolar surfaces in the folding of *Escherichia coli* dihydrofolate reductase detected by 1-anilinonaphthalene-8-sulfonate binding. *Biochemistry* **33**, 15250-15258
34. Yutani, K., Ogasahara, K., Tsujita, T., and Sugino, Y. (1987) Dependence of conformational stability on hydrophobicity of the amino acid residue in a series of variant proteins substituted at a unique position of tryptophan synthase α subunit. *Proc. Natl. Acad. Sci. USA* **84**, 4441-4444
35. Matsumura, M., Becktel, W.J., and Matthews, B.W. (1988) Hydrophobic stabilization in T4 lysozyme determined directly by multiple substitutions of Ile 3. *Nature* **334**, 406-410
36. Matsumura, M., Yahanda, S., Yasumura, S., Yutani, K., and Aiba, S. (1988) Role of tyrosine-80 in the stability of kanamycin nucleotidyltransferase analyzed by site-directed mutagenesis. *Eur. J. Biochem.* **171**, 715-720
37. Kellis, J.T., Nyberg, K., and Fersht, A.R. (1989) Energetics of complementary side-chain packing in a protein hydrophobic core. *Biochemistry* **28**, 4914-4922
38. Kauzmann, W. (1959) Some factors in the interpretation of protein denaturation. *Adv. Protein Chem.* **14**, 1-63
39. Lim, W.A., Farruggio, D.C., and Sauer, R.T. (1992) Structural and energetic consequences of disruptive mutations in a protein core. *Biochemistry* **31**, 4324-4333
40. Shortle, D., Stites, W.E., and Meeker, A.K. (1990) Contributions of the large hydrophobic amino acids to the stability of staphylococcal nuclease. *Biochemistry* **29**, 8033-8041
41. Green, S.M., Meeker, A.K., and Shortle, D. (1992) Contributions of the polar, uncharged amino acids to the stability of staphylococcal nuclease: Evidence for mutational effects on the free energy of the denatured state. *Biochemistry* **31**, 5717-5728
42. Green, S.M. and Shortle, D. (1993) Patterns of nonadditivity between pairs of stability mutations in staphylococcal nuclease. *Biochemistry* **32**, 10131-10139
43. Pakula, A.A. and Sauer, R.T. (1990) Reverse hydrophobic effects relieved by amino-acid substitutions at a protein surface. *Nature* **344**, 363-364
44. Bowler, B.E., May, K., Zaragoza, T., York, P., Dong, A., and Caughey, W.S. (1993) Destabilizing effects of replacing a surface lysine of cytochrome *c* with aromatic amino acids: Implications for the denatured state. *Biochemistry* **32**, 183-190
45. Nozaki, Y. and Tanford, C. (1971) The solubility of amino acids and two glycine peptides in aqueous ethanol and dioxane solutions. *J. Biol. Chem.* **246**, 2211-2217
46. Baum, J., Dobson, C.M., Evans, P.A., and Hanley, C. (1989) Characterization of a partly folded protein by NMR methods: Studies on the molten globule state of guinea pig α-lactalbumin. *Biochemistry* **28**, 7-13
47. Tamura, Y. and Gekko, K. (1995) Compactness of thermally and chemically denatured ribonuclease A as revealed by volume and compressibility. *Biochemistry* **34**, 1878-1884
48. Gekko, K. and Hasegawa, Y. (1986) Compressibility-structure relationship of globular proteins. *Biochemistry* **25**, 6563-6571
49. Shellman, J.A. (1978) Solvent denaturation. *Biopolymers* **17**, 1305-1322
50. Pace, C.N., Laurents, D.V., and Thomson, J.A. (1990) pH dependence of the urea and guanidine hydrochloride denaturation of ribonuclease A and ribonuclease T1. *Biochemistry* **29**, 2564-2572
51. Zamyatnin, A.A. (1984) Amino acid, peptide, and protein volume in solution. *Annu. Rev. Biophys. Bioeng.* **13**, 145-165